The Best Objective Function for Seeded Batch Crystallization

Che-Wei Hsu and Jeffrey D. Ward
Dept. of Chemical Engineering, National Taiwan University, Taipei 106-07, Taiwan

DOI 10.1002/aic.13855

Although many researchers have optimized the operation of seeded batch crystallization, there remains little understanding of the effect of the choice of objective function on the optimization and no consensus on which objective function is best. In this work, different objective functions for seeded batch crystallization are compared by calculating the supersaturation trajectory that minimizes each objective function and then comparing the results of each trajectory. We show that some objective functions lead to trajectories that cause excessive nucleated mass and should be avoided. We conclude that the best objective function in most cases is to minimize the nucleated mass. This also corresponds to maximizing the growth of seeds, and leads to a product with a large volume mean size. We also show that the width of the product crystal size distribution can be controlled much more effectively by manipulating seed properties than by adjusting the supersaturation trajectory. © 2012 American Institute of Chemical Engineers *AIChE J,* 59: 390–398, 2013
Keywords: crystal growth (industrial crystallization), optimization, particle technology

Introduction

Batch crystallization is a widely used method for separation and purification of chemicals, as well as the preparation of solid products. In a typical operation, a solution with a high concentration of solute is prepared, seeds are added, and then the solubility of the solute is gradually reduced (by cooling, solvent evaporation, or some other method). As the solubility is reduced, the solution becomes supersaturated, and this supersaturation provides the driving force for crystal growth. If the supersaturation is maintained within the metastable limit, primary nucleation does not occur, but nuclei may still form via secondary mechanisms. As both the nucleation rate and the crystal growth rate increase with increasing supersaturation, there is an inherent tradeoff between these phenomena.

In most batch crystallization processes, seeds are introduced at the beginning of the batch, and the process is therefore called seeded batch crystallization. The reason for introducing seeds is to improve the product crystal size distribution. If the supersaturation is relieved via the growth of seeds, then the crystallization proceeds in a controlled way. If the seed crystal size distribution (CSD) is narrow, then the product CSD will also be narrow, and the product crystals will have an average size that can be predicted by material balance. If an inadequate mass of seeds is used, or if a poor choice is made for the temperature–time trajectory, then a significant fraction of the mass of solute crystallized may be consumed in the growth of small nuclei that form during the batch. In this case, the product CSD will be bimodal, with one mode corresponding to the seeds and another mode corresponding to the nucleated crystals. This is almost always undesirable.

Therefore, when seeds are used, the real operational objective for the process is almost always to maximize the growth of seeds while minimizing the amount of solute consumed in the growth of nucleated crystals. If small product crystals are desired (say 10 μm) then seeds of an even smaller size should be used, and an adequate number of seeds should be used, so that the seeds grow to the desired final size when all of the solute is consumed in their growth according to the material balance.

A commonly studied problem related to seeded batch crystallizer operation is the determination of an optimal temperature, saturation concentration, or crystal growth rate trajectory. Although it is well understood that the optimization involves a tradeoff between nucleation and growth and that growth is desirable whereas nucleated crystals are undesirable, a survey of the literature shows that many different objective functions have been used by different authors to identify saturation concentration trajectories. Table 1 provides an incomplete list of journal articles in which an optimal saturation concentration trajectory is determined based on an objective that is formulated in terms of the final moments of the CSD (either seed crystals, nucleated crystals, or a combination of these). There are more than 10 different objectives reported in 22 different articles.[1–23] Many of these objective functions can be classified into one of three broad groups: those that aim to maximize a product average size (either the number-average size or weight-average size), those that aim to maximize a moment of the seed crystals or minimize a moment of the nucleated crystals, and those that attempt to minimize a coefficient of variation (either the number coefficient of variation or the mass coefficient of variation).

Although several authors have considered more than one objective function,[15–23] we are not aware of any that have compared the results from different objective functions in a critical way or offered a suggestion as to which objective

---

Correspondence concerning this article should be addressed to J. D. Ward at jeffward@ntu.edu.tw.

Table 1. Objective Functions Used in Literature Reports

Objective to Minimize	Reference	Objective to Minimize	Reference
$\mu_{\mathrm{n}3}$	1	$-\frac{\mu_4}{\mu_3} + 0.0005\sqrt{\frac{\mu_5\mu_3}{\mu_4^2} - 1}$	13
$\mu_{\mathrm{n}3}$	2	$0.00081\frac{\mu_4}{\mu_3} + 0.025\frac{\mu_3}{\mu_{\mathrm{s}3}} - 0.10\sqrt{\frac{\mu_2\mu_0}{\mu_1^2}} - 1$	14
$\frac{\mu_2}{\mu_0} - \left(\frac{\mu_1}{\mu_0}\right)^2 - \alpha\left(\frac{\mu_1}{\mu_0}\right)$	3	$-\frac{\mu_4}{\mu_3}, \left(\frac{\mu_2\mu_0}{\mu_1^2} - 1\right)^2$	15
$\frac{\mu_{\mathrm{n}3}}{\mu_{\mathrm{s}3}}$	4	$\frac{\mu_{\mathrm{n}3}}{\mu_{\mathrm{s}3}}, \sqrt{\frac{\mu_5\mu_3}{\mu_4^2}} - 1$	16
$\mu_{\mathrm{s}1}$	5	$\frac{\mu_{\mathrm{n}3}}{\mu_{\mathrm{s}3}}, \sqrt{\frac{\mu_5\mu_3}{\mu_4^2}} - 1$	17
$-\frac{\mu_1}{\mu_0}$	6	$-\frac{\mu_4}{\mu_3}, \mu_{\mathrm{n}3}, \sqrt{\frac{\mu_5\mu_3}{\mu_4^2}} - 1$	18
$\mu_{\mathrm{n}3} - \mu_{\mathrm{s}3} - \mu_{\mathrm{n}3}$	7	$-\frac{\mu_4}{\mu_3}, \sqrt{\frac{\mu_5\mu_3}{\mu_4^2} - 1}, -\frac{\mu_4}{\mu_3} - \frac{\alpha}{t_{\mathrm{f}}}$	19
$-\frac{\mu_1}{\mu_0}$	8	$-\frac{\mu_4}{\mu_3}, \sqrt{\frac{\mu_5\mu_3}{\mu_4^2} - 1}$	20
$\mu_{\mathrm{n}3}$	9	$-\frac{\mu_4}{\mu_3}, \frac{\mu_{\mathrm{n}3}}{\mu_{\mathrm{s}3}}$	21
$-\frac{\mu_4}{\mu_3}$	10	$-\frac{\mu_4}{\mu_3}, \sqrt{\frac{\mu_2\mu_0}{\mu_1^2}} - 1, \frac{\mu_{\mathrm{n}3}}{\mu_{\mathrm{s}3}}$	22
$-\frac{\mu_4}{\mu_3}$	11	$-\frac{\mu_4}{\mu_3}, \sqrt{\frac{\mu_2\mu_0}{\mu_1^2}} - 1, \frac{\mu_{\mathrm{n}3}}{\mu_{\mathrm{s}3}}$	23
$-\frac{\mu_4}{\mu_3}$	12		

function is the best. That is the purpose of this work. We compare different objective functions by comparing the resulting final product crystal size distribution when different objective functions are used to determine the saturation concentration trajectory.

Based on the results, we conclude that the best objective function for almost all applications is to minimize the nucleated mass. This objective is closely correlated with maximizing the product average crystal size. Minimizing the number of nuclei formed or a total product coefficient of variation leads (somewhat unexpectedly) to an excess of nucleated mass and is therefore undesirable. We also show that the product coefficients of variation (mass and number) can both be easily improved by adjusting the seed properties.

Model Development and Optimization

The crystallization process model used in this work is the dimensionless model originally presented by Ward et al.[1] This model has the advantage that it is not particular to any solute–solvent system. The key equations are presented here, and the reader is referred to Ward et al.[1] for the details.

The population balance equation for a well-mixed batch crystallizer with no agglomeration or breakage is

$$\frac{\partial f(L,t)}{\partial t} + \frac{\partial (G(L,t)f(L,t))}{\partial L} = 0 \qquad (1)$$

where $f(L, t)$ is the CSD function, and G is the crystal growth rate (m/s). Equation 1 is subject to an initial condition based on the properties of the seeds at the beginning of the batch, and to a left boundary condition

$$f(0,t) = \frac{B(f(L,t),t)}{G(0,t)} \qquad (2)$$

where B is the nucleation rate. The driving force for both nucleation and growth is the supersaturation

$$S = C - C_{\mathrm{sat}} \qquad (3)$$

Common forms for the expressions for crystal growth rate and secondary nucleation are

$$G = k_{\mathrm{g}}S^{g} \qquad (4)$$

$$B = k_{\mathrm{b}}G^{\gamma}\mu_3 \qquad (5)$$

where k_{g}, g, k_{b}, and i are empirically determined kinetic parameters, and μ_3 is the third moment of the CSD. The moments of the CSD are determined according to

$$\mu_i = \int_0^{\infty} L^i f(L)dL \quad i = 0,1,2,... \qquad (6)$$

Moments of the seed-grown and nucleated crystals are represented by $\mu_{\mathrm{n}i}$ and $\mu_{\mathrm{s}i}$, respectively. A material balance on the solute shows that:

$$\frac{dC}{dt} = -3\rho_{\mathrm{c}}k_{\mathrm{v}}\mu_2 \qquad (7)$$

With a suitable choice of dimensionless variables (see Table 2 and Ward et al.[1] for further details), the following dimensionless model can be obtained

$$\frac{d\mu_0'}{dt} = B' = (G')^{\gamma}\mu_3' \qquad (8)$$

$$\frac{d\mu_i'}{dt} = G'\mu_{i-1}' \; i = 1,2,\cdots \qquad (9)$$

$$C' = 1 + m_{\mathrm{s}}' - \mu_3' \qquad (10)$$

Over the course of the batch, C' decreases from 1 to 0, whereas μ'_3 increases from m'_{s} to $m'_{\mathrm{s}} + 1$. Using this model, the dimensionless growth rate trajectory $G'(t')$ that minimizes an objective function that depends on the properties of the dimensionless moments at the end of the batch can be determined.

The initial seed crystal size distribution is parabolic (as discussed by Ward et al.[1]) with dimensionless width $w' = 1$, seed mean size $x'_0 = 1.5$, and dimensionless seed mass $m'_{\mathrm{s}} = 0.1$. The growth rate trajectory that minimized each objective function was determined using the simulated annealing toolbox in Matlab. The growth rate trajectory was specified by a piece-wise linear spline with 25 points. For all objective functions, a production rate constraint was imposed that required the dimensionless concentration to reach zero at the end of the batch.

Note that the temperature of the crystallizer does not appear explicitly in the model. This does not mean that the

Table 2. Definition of Reference Variables

Reference Variable	Definition
$\bar{G}$	$(k_{\mathrm{b}}t_{\mathrm{f}}^4)^{\frac{-1}{\gamma+3}}$
$\bar{B}$	$\frac{k_{\mathrm{b}}(C_0 - C_{\mathrm{f}})}{\rho k_{\mathrm{v}}}(k_{\mathrm{b}}t_{\mathrm{f}}^4)^{\frac{-\gamma}{\gamma+3}}$
$\bar{\mu}_i$	$\bar{B}\bar{G}^{i}t_{\mathrm{f}}^{i+1}$
$\bar{f}$	$\frac{\bar{G}f}{\bar{B}}$

Table 3. Weight COV and Number COV of All Crystals and Seed Crystals When Weight COV and Number COV Are Minimized

	Min wCOV	Min #COV
wt COV	0.397	0.729
# COV	1.52	0.328
wt COVs	0.0740	0.0917
# COVs	1.00	1.01

crystallizer temperature must be constant, only that the rates of nucleation and growth do not depend strongly on the temperature. If the crystallizer is a cooling crystallizer, then one can solve for the temperature trajectory $T(t)$ that will lead to the desired supersaturation trajectory $S(t)$. If the crystallizer operates by evaproation, antisolvent addition, or some other mechanism, then one can solve for the trajectory of the manipulated variable that will lead to the desired supersaturation trajectory $S(t)$.

This dimensionless model is based on the msot commonly used models for the kinetics of crystal nucleation and growth (Eqs. 4 and 5). Because the model parameters are combined to form dimensionless groups, by investigating a range of dimensionless parameters we can consider a wide range of realistic process conditions for different solute–solvant systems. Thus, the results should be valid for msot processes where the kinetics of nucleation and growth are similar to those of Eqs. 4 and 5.

Results

Minimizing coefficients of variance

The coefficient of variation (COV) of the product crystal size distribution can be expressed in terms of the moments as

$$\#\mathrm{COV} = \sqrt{\frac{\mu_2\mu_0}{\mu_1^2} - 1} \tag{11}$$

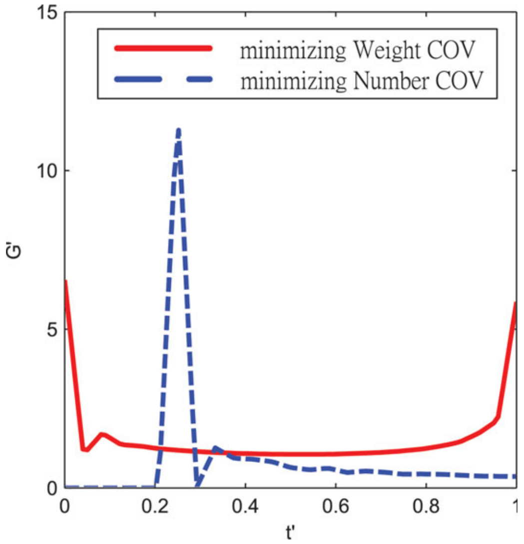

Figure 1. Growth rate trajectories that minimize the weight coefficient of variation and the number coefficient of variation.

[Color figure can be viewed in the online issue, which is available at wileyonlinelibrary.com.]

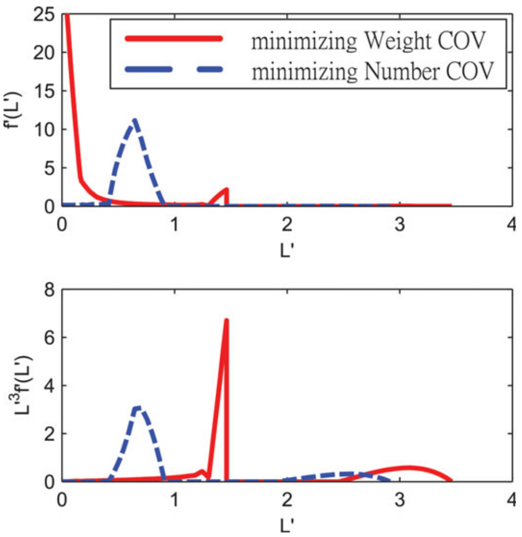

Figure 2. Final number and volume crystal size distributions when weight COV and number COV are minimized.

[Color figure can be viewed in the online issue, which is available at wileyonlinelibrary.com.]

The coefficient of variation of the product volume (or weight) distribution can be expressed in terms of the moments as

$$\mathrm{wt\,COV} = \sqrt{\frac{\mu_5\mu_3}{\mu_4^2} - 1} \tag{12}$$

The number and weight COV of both the total crystal product (seeds and nuclei) and the seeds alone when minimizing the weight COV and number COV are shown in Table 3. The growth rate trajectory and resulting number and volume size distributions are shown in Figures 1 and 2, respectively. When the objective is to minimize the weight COV, the resulting values of the weight COV and number COV are 0.397 and 1.52, respectively. (All values are dimensionless, because the moments themselves are dimensionless in the dimensionless model.) When the objective is to minimize the number COV, the values of the weight COV and number COV are 0.729 and 0.328, respectively. Both optimizations work as desired in the sense that the weight COV is indeed minimized when this is the objective, and the number COV is indeed minimized when minimizing the number COV is the objective. However, there is an inherent tradeoff: when the weight COV is minimized, the number COV is significantly higher than the minimum possible value, and when the number COV is minimized, the weight COV is significantly higher than the minimum possible value.

The last two rows in Table 3 show the weight COV and number COV of the seeds only. As minimizing the weight COV causes the seeds to grow to a larger size than minimizing the number COV, the seed weight COV is smaller when the weight COV is minimized than when the number COV is minimized. However, the seed number COV is unchanged, because the shape of the number CSD of the seeds is not affected by the growth rate trajectory. For these reasons, we conclude that minimizing the weight COV is a superior objective to minimizing the number COV.

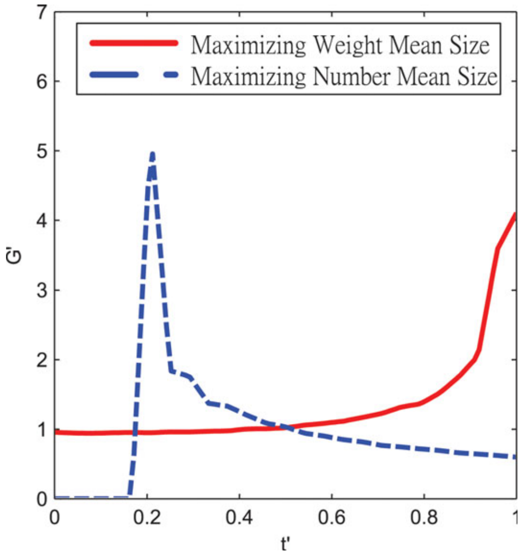

Figure 3. Growth rate trajectories that maximize the weight mean size and number mean size.

[Color figure can be viewed in the online issue, which is available at wileyonlinelibrary.com.]

Maximizing weight mean size

The second set of objective functions that we consider includes those that aim to maximize a combined mean size, either the weight mean size (WMS) (μ'_4/μ'_3) or number mean size (NMS) (μ'_1/μ'_0). Figure 3 shows the resulting growth rate trajectory for these two objective functions. Maximizing the number mean size also results in a growth rate trajectory with a large spike at the beginning of the batch. Figure 4 shows that this again results in a large nucleated mass at the end of the batch. The number mean size is maximized by growing a large number of nuclei to the largest possible size, instead of growing the seeds. Again this is not really the desired behavior: one presumes that the real goal when using this objective is to maximize the number mean size by growing the seeds as large as possible.

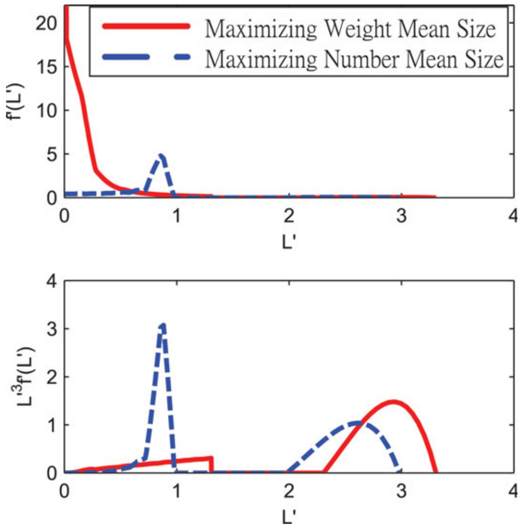

Figure 4. Final number and volume crystal size distributions when the weight mean size and number mean size are maximized.

[Color figure can be viewed in the online issue, which is available at wileyonlinelibrary.com.]

Table 4. WMS and NMS of All Crystals and Seed Crystals When WMS and NMS Are Minimized

	Max WMS	Max NMS
WMS	2.395	1.62
NMS	0.235	0.771
WMSs	3.04	2.61
NMSs	2.99	2.55

Maximizing the weight mean size results in a trajectory very similar to that obtained when minimizing the third moment of the nuclei, as will be shown later. Table 4 shows the values of the weight mean size and number mean size when these two objective functions are used. When the objective is to maximize the weight mean size, the resulting values of the weight mean size and number mean size are 2.40 and 0.235, respectively.

Minimizing a moment of the nuclei

The final category of objective functions considered in this work includes those that aim to minimize a moment of the nuclei (0–3). We are not aware of any researchers that attempt to minimize the second moment of the nuclei, but it is included for completeness. Figure 5 shows the growth rate trajectories that result from each of these objective functions. A clear trend is evident: as the moment used in the objective function increases, the spike in the growth rate at the beginning of the batch decreases in height, and the spike in the growth rate at the end of the batch increases. This trend can be understood in terms of the arguments about ‘‘early growth’’ and ‘‘late growth’’ trajectories presented earlier by Ward et al.[24]

The nucleation rate depends on both the supersaturation and the total solid mass in the system. The number of nuclei can be minimized using a higher growth rate at the beginning of the batch, when the solid mass is the least. However, this will result in a larger mass of nucleated crystals, because nuclei that are formed at the beginning of the batch have a longer time to grow. Conversely, the mass of nuclei can be

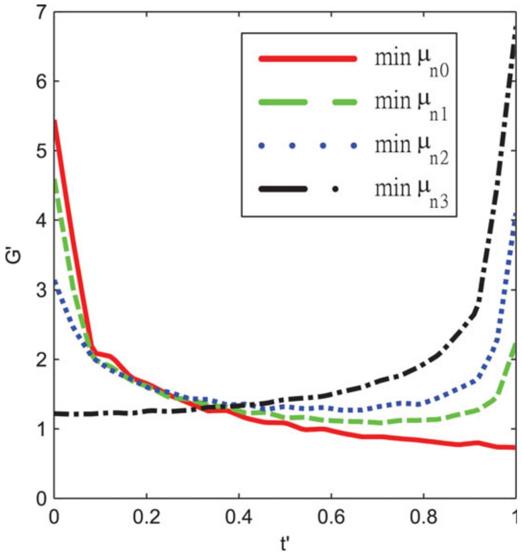

Figure 5. The growth rate trajectories that minimize the dimensionless moments.

[Color figure can be viewed in the online issue, which is available at wileyonlinelibrary.com.]

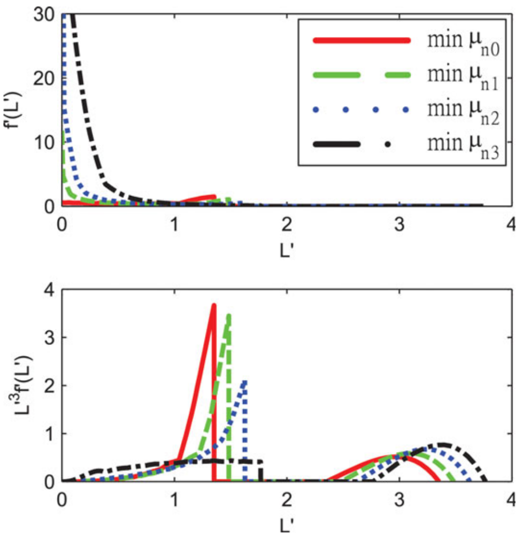

Figure 6. Final number and volume crystal size distributions when the dimensionless moments are minimized.

[Color figure can be viewed in the online issue, which is available at wileyonlinelibrary.com.]

minimized using a higher growth rate at the end of the batch. Although more nuclei will be formed (because the total crystal mass is larger), those nuclei that are formed will not have a chance to grow to a large size.

Figure 6 shows the number and mass distributions when different moments of the nucleated crystals are minimized. There is clearly a tradeoff: when the number of nuclei is minimized, the nucleated mass is greater and the seeds grow to a smaller size. This is reflected by the fact that the parabola corresponding to the seeds in the volume distribution plot is shifted less far to the right. Although there may be some cases where it is desirable to minimize the number of nuclei, we feel that in most cases, the best objective is to minimize the mass of nuclei, which also corresponds to maximizing the growth of the seeds.

Note also that as all of the seeds grow at the same rate, all of the seed moments are related and maximizing any moment of the seeds (other than the zeroth, which does not change) is equivalent to maximizing the third moment of the seeds, which is equivalent to minimizing the third moment of the nuclei, by material balance.

Table 5 shows the values of all of the moments of the nuclei and seeds when each moment of the nuclei is minimized. Again a tradeoff is clear: when the zeroth moment of the nuclei (the number of nuclei) is minimized, the volume (mass) of the nuclei is much larger than necessary. However, when the third moment of the nuclei is minimized, all of the moments of the seeds are maximized. This is required by material balance, as discussed earlier. Therefore, we conclude that among the objectives that minimize a moment of the nuclei, the most suitable choice is to minimize the third moment of the nuclei.

Table 5. Moments of the Seeds and Nuclei When Each Moment of the Nuclei Is Minimized

	Min μ'_{n0}	Min μ'_{n1}	Min μ'_{n2}	Min μ'_{n3}
μ'_{n0}	0.776	1.10	2.31	6.68
μ'_{n1}	0.559	0.494	0.584	1.18
μ'_{n2}	0.523	0.433	0.397	0.488
μ'_{n3}	0.534	0.452	0.380	0.341
μ'_{s0}	0.0278	0.0278	0.0278	0.0278
μ'_{s1}	0.0754	0.0789	0.0817	0.0832
μ'_{s2}	0.206	0.225	0.242	0.251
μ'_{s3}	0.566	0.648	0.720	0.759

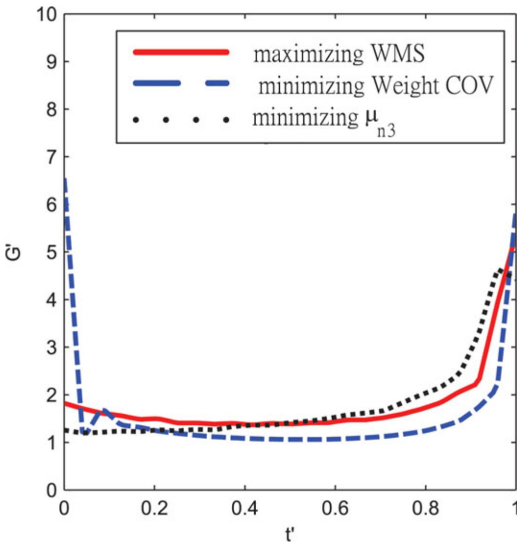

Figure 7. The growth rate trajectories for three cases: minimizing the nucleated mass, minimizing weight coefficient of variation, and maximizing weight mean size.

[Color figure can be viewed in the online issue, which is available at wileyonlinelibrary.com.]

Comparing the best objective from each category

Finally, we compare the best objective function from each category to determine which is the best overall. Figure 7 shows the growth trajectories for three cases: maximizing the weight mean size, minimizing the weight COV, and minimizing μ'_{3n}. The trajectories for maximizing the WMS and minimizing μ'_{3n} are qualitatively similar, whereas the trajectory that minimizes the weight COV is qualitatively quite different, having a large peak at the beginning of the batch as well as at the end of the batch.

The result of this is shown in Figure 8, which shows the number and volume crystal size distributions for the three cases. The distributions for the case of maximizing the weight mean size and minimizing μ'_{3n} are similar, while the distribution with the minimum weight coefficient of variation has a large mass of nuclei (the peak at $L' \approx 1.4$) and a reduced seed mass. This results in a lower mass coefficient of variation, because the nuclei peak is closer to the seed peak but is not the desired behavior, as there is an excessive mass of nucleated crystals, and the growth of the seeds is reduced.

Table 6 shows the actual values of the WMS, weight COV, and μ'_{3n}, as well as the seed WMS, seed weight COV, and μ'_{3s} for the cases where the WMS is maximized, the weight COV is minimized and μ'_{3n} is minimized. Again, maximizing the weight mean size and minimizing μ'_{3n} give similar results, but considering the seed properties, minimizing μ'_{3n} does slightly better, because the seed weight mean size is identical to three significant figures, but the third moment of the seeds is slightly larger when the third moment of the nuclei is minimized. Furthermore, minimizing the nucleated mass is easier to justify intuitively as an

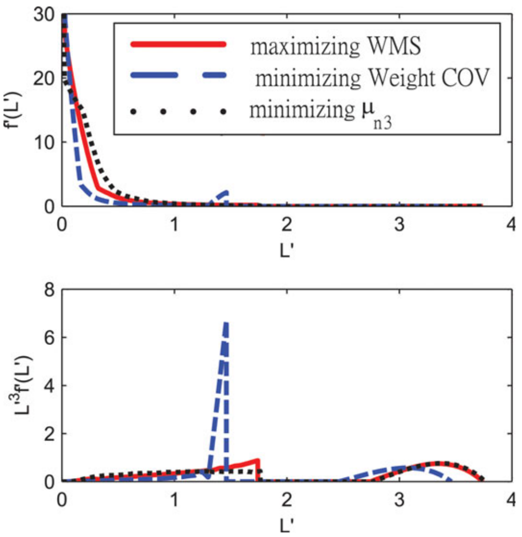

Figure 8. Final number and volume crystal size distributions for three cases: when the nucleated mass is minimized, when weight coefficient of variation is minimized, and when weight mean size is maximized.

[Color figure can be viewed in the online issue, which is available at wileyonlinelibrary.com.]

objective function, because it corresponds to maximizing the growth of seeds and at the same time minimizing the nucleated mass. Therefore, we recommend minimizing the nucleated mass as the best objective for determining the temperature or growth rate trajectory for batch crystallization.

Achieving a narrow product distribution by adjusting seed properties

It was shown earlier that minimizing the nucleated mass also results in a product weight mean size that is near to the maximum possible weight mean size, however, the weight coefficient of variance is significantly higher than the minimum achievable. In this section, we show that the weight coefficient of variance can be minimized much more effectively by manipulating seed properties rather than adjusting the growth rate trajectory. The problem is, if the seed distribution is broad, it is impossible to produce a product distribution that is narrow. The crystal size distribution from a seeded batch crystallizer is inherently bimodal, with one peak corresponding to the seeds and another corresponding to the nuclei. (If a sufficiently large seed mass is used, the peak corresponding to the nuclei can be made small enough that it is not detectable in the laboratory,[25–27] but theory and computer simulations still predict its existence.)

If the seed crystal size distribution is broad, a computer algorithm attempting to minimize the weight coefficient of variation will produce a growth trajectory that causes a surge of nucleation at the beginning of the batch. This has two effects: this large number of nuclei grows to a large size and therefore there is a large nucleated mass, and the seeds grow to a smaller size. The result is that the peak associated with the nuclei and the peak associated with the seeds are closer together, which reduces the weight coefficient of variation. However, this is clearly not the desired result, because the resulting crystal size distribution is still bimodal and indeed the peak associated with the nuclei may have a greater mass than the peak associated with the seeds.

This phenomenon is demonstrated in this section. Figure 9 shows a set of different parabolic initial crystal size distributions with different widths and seed masses. All of the distributions have the same initial size $L' = 1.5$. Figure 10 shows the resulting volume size distribution when the mass coefficient of variation is minimized. When the seed distribution is narrow (in the upper left panel in the diagram), there is relatively little nucleated mass, especially when the initial seed mass is the largest. As the width of the seed distribution increases, the algorithm increasingly prefers growth rate trajectories that lead to a greater nucleated mass.

Therefore, we conclude that the best strategy for achieving a final product crystal size distribution with a large mean crystal size, narrow crystal distribution, maximal seed growth and minimal nucleated mass is to start with a narrow seed distribution, use a sufficient seed mass to control nucleation, and use a growth rate trajectory that minimizes the nucleated mass at the end of the batch.

Comments

Composite objective functions and Pareto-optimal fronts

Some authors have sought to address the problem of competing objectives by developing composite objective functions that are the sum of two or more objective functions suitably weighted.[3,13,14] Others have constructed the Pareto-optimal front for two or more different objective functions.[18] Although these methods have merit, they also have drawbacks. If a composite objective function is to be developed, the engineer must decide which objective functions to include and what weights to assign to them. If a Pareto-optimal front is to be determined, the engineer must also decide which objective functions to use, and the construction of a Pareto-optimal front is much more computationally intensive than determining a single optimal trajectory. Finally, even after a Pareto-optimal front is constructed, the engineer must still choose a point along the front at which to operate.

For these reasons, we feel that in most cases, and especially for rapid process development, it is preferable to follow the procedure recommended in this article, namely to use minimizing the nucleated mass as the objective for determining the growth rate trajectory, use an adequate seed mass to suppress nucleation to the desired degree, and control the product distribution by adjusting the seed distribution.

The Mullin–Nyvlt trajectory

There is a further advantage of using minimizing the nucleated mass as the objective function for seeded batch crystallization: the growth rate trajectory that minimizes the nucleated mass is very similar to the analytical trajectory first proposed by Mullin and Nyvlt.[28] The Mullin–Nyvlt trajectory is derived on the basis of the assumption that the crystal growth rate is constant and the nucleated mass does

Table 6. WMS, Weight COV and Third Moment of Nuclei When WMS, Weight COV and Third Moment of Nuclei Are Minimized

	Max WMS	Min wCOV	Min μ'_{n3}
WMS	2.40	2.31	2.39
wCOV	0.0287	0.0247	0.0330
μ'_{n3}	0.346	0.395	0.342
WMSs	3.04	2.97	3.04
wCOVs	0.0725	0.0740	0.0723
μ'_{s3}	0.754	0.706	0.759

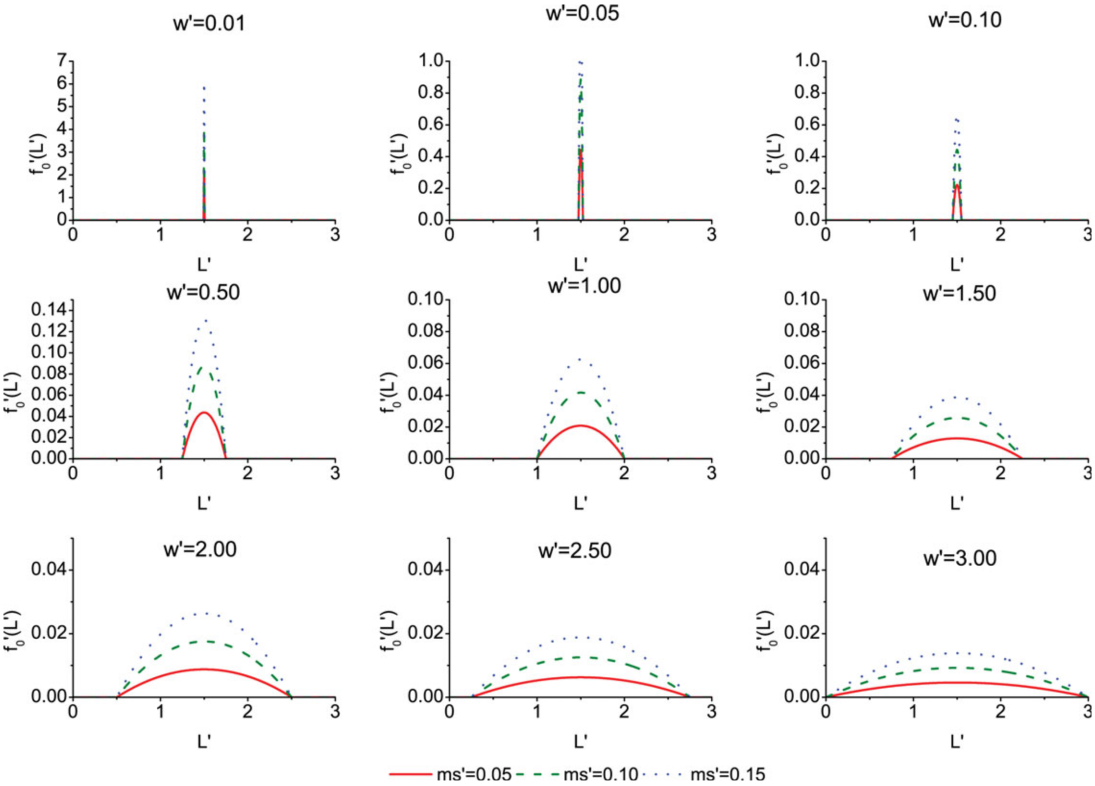

Figure 9. Initial crystal size distributions used to investigate the effect of seed distribution on final product coefficients of variation.

[Color figure can be viewed in the online issue, which is available at wileyonlinelibrary.com.]

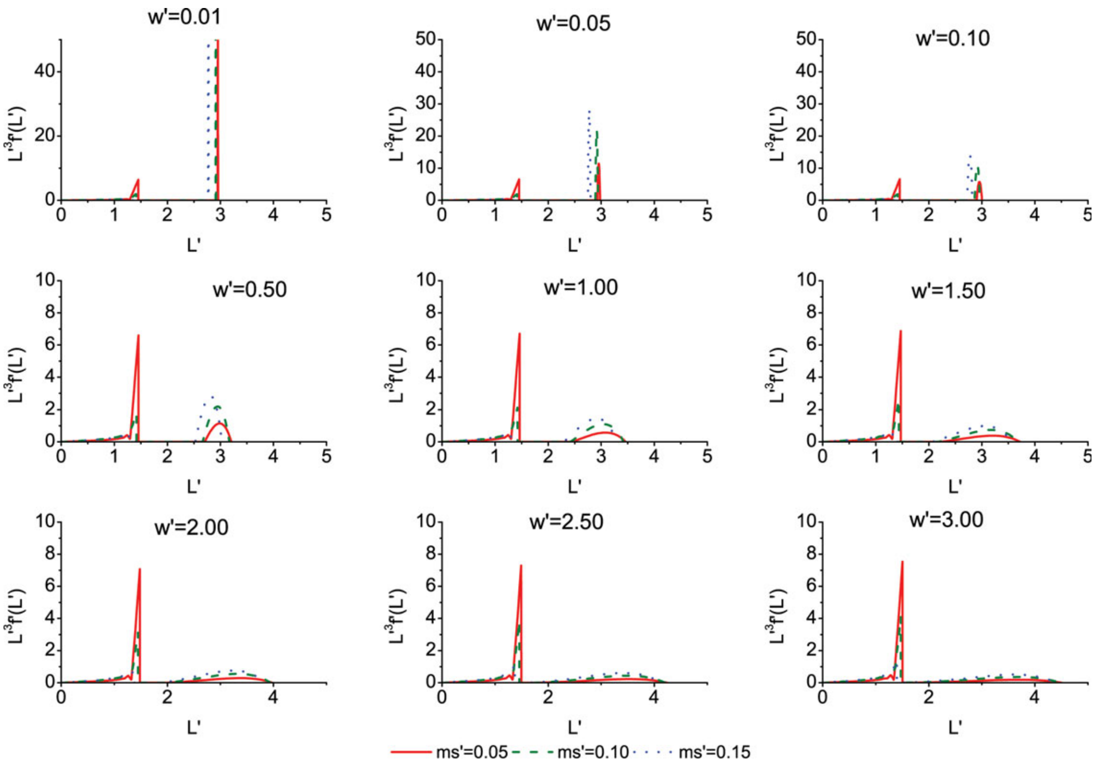

Figure 10. Final crystal size distributions when weight coefficient of variation is minimized starting with different seed distributions.

[Color figure can be viewed in the online issue, which is available at wileyonlinelibrary.com.]

not make a significant contribution to the overall material balance. This trajectory can be expressed analytically in terms of the seed mass, the initial and final solution concentration, and the batch time. It does not depend on any kinetic parameters such as k_g, k_b, etc. Ward, et al.[1] showed that in almost all cases, this trajectory performs almost as well as the optimal trajectory at minimizing the nucleated mass.

Thus using this method it is possible to come near to the optimal operating recipe for a seeded batch crystallizer without even developing a kinetic model for crystal nucleation and growth or conducting any kind of optimization at all, and without measuring supersaturation online. One can simply use the Mullin–Nyvlt trajectory in conjunction with a seed loading of adequate mass and narrow distribution to achieve a nearly unimodal, narrow product distribution with large average crystal size, maximal seed growth, and minimal nucleated mass.

Conclusions

In this article, we argue that the best objective function for seeded batch crystallization in most cases is to minimize the nucleated mass, which is equivalent to maximizing the growth of seeds. To support this claim, we determine the growth rate trajectories that minimize a number of different objective functions used by other researchers and compare the results. Some objective functions, such as minimizing the weight or number coefficient of variation, or the number of nuclei, lead to an excessive nucleated mass and less crystal growth, which is presumably not the desired result.

If an objective other than minimizing the nucleated mass is used, one is in effect deliberately causing extra, unnecessary nucleated mass in the hopes that the nuclei will somehow combine together with the seed crystals to improve the overall crystal size distribution. In some cases, this may lead to a better value of some objective functions, but it is unlikely to lead to a real improvement in process performance. If a narrow product CSD is desired, it is more reasonable to start with a narrow seed CSD and grow the seeds to a larger size than to start with a broad seed CSD and attempt to correct the problem using the saturation concentration trajectory. If a different shape of product crystal size distribution is desired (such as rectangular, trapezoidal, and something else) it is most reasonable to start the batch with seeds that have the desired distribution shape but a smaller size and grow them to a larger size.

Acknowledgments

The authors gratefully acknowledge financial support from the National Science Council of Taiwan.

Notation

B = nucleation rate, #/(m^3 s)
f = crystal size distribution function, #/m^3 m
G = crystal growth rate, m/s
g = growth parameter
i = nucleation parameter
k_b = nucleation parameter, 1/(m^3 s)(m/s)$^{-i}$
k_g = growth parameter, (m/s) (kg/m^3)$^{-g}$
k_v = volumetric shape factor
C = concentration, kg/m^3
S = supersaturation, kg/m^3
μ_i = ith moment of the crystal size distribution, m^i/m^3
ρ = crystal density, kg/m^3

Notes: an overbar indicates a dimensional reference quantity and a prime indicates a dimensionless quantity. Variables are made dimensionless by dividing by the reference quantity, that is, $G' = G/\bar{G}$. When it is necessary to distinguish moments of the seed-grown crystals from moments of nucleus-grown crystals, a double subscript is used with the letter "s" or "n," respectively, together with the moment number, that is, μ_{3n} is the third moment of the nucleus-grown crystals.

Literature Cited

1. Ward JD, Yu CC, Doherty MF. A new framework and a simpler method for the development of batch crystallization recipes. *AIChE J*. 2011;57(3):606–617.
2. Rawlings JB, Miller SM, Witkowski WR. Model identification and control of solution crystallization processes: a Review. *Ind Eng Chem Res*. 1993;32:1275–1296.
3. Chang CT, Epstein MAF. *Identification of batch crystallization control strategies using characteristic curves*. In: Epstein MAF, editor. *Nucleation, Growth and Impurity Effects in Crystallization Process Engineering*. New York: AIChE, 1982.
4. Eaton JW, Rawlings JB. Feedback control of chemical processes using on-line optimization techniques. *Comput Chem Eng*. 1990;14:469–479.
5. Jones AG. Optimal operation of a batch cooling crystallizer. *Chem Eng Sci*. 1974;29:1075–1087.
6. Ma DL, Braatz RD. Robust identification and control of batch processes. *Comput Chem Eng*. 2003;27:1175–1184.
7. Paengjuntuek W, Kittisupakom P, Arpomwichanop A. Optimization and nonlinear control of a batch crystallization process. *J Chin Inst Chem Eng*. 2008;39(3):249–256.
8. Braatz RD, Nagy ZK, Chew JW, Fujiwara M. Comparative performance of concentration and temperature controlled batch crystallizations. *J Process Control*. 2008;18(3–4):399–407.
9. Shi D, El-Farra NH, Li MH, Mhaskar P, Christofides PD. Predictive control of particle size distribution in particulate processes. *Chem Eng Sci*. 2006;61(1):268–281.
10. Yang AD, Montague G, Martin EB. Importance of heterogeneous energy dissipation in the modeling and optimization of batch cooling crystallization. *Ind Eng Chem Res*. 2007;46(22):7177–7187.
11. Choong KL, Smith R. Novel strategies for optimization of batch, semi-batch and heating/cooling evaporative crystallization. *Chem Eng Sci*. 2004;59(2):329–343.
12. Shi D, Mhaskar P, El-Farra NH, Christofides PD. Predictive control of crystal size distribution in protein crystallization. *Nanotechnology*. 2005;16(7):S562–S574.
13. Zhang GP, Rohani S. On-line optimal control of a seeded batch cooling crystallizer. *Chem Eng Sci*. 2003;58(9):1887–1896.
14. Ge M, Wang QG, Chiu MS, Lee TH, Hang CC, Teo KH. An effective technique for batch process optimization with application to crystallization. *Chem Eng Res Des*. 2000;78(A1):99–106.
15. Chung SH, Ma DL, Braatz RD. Optimal seeding in batch crystallization. *Can J Chem Eng*. 1999;77:590–596.
16. Sheikhzadeh M, Trifkovic M, Rohani S. Real-time optimal control of an anti-solvent isothermal semi-batch crystallization process. *Chem Eng Sci*. 2008;63(3):829–839.
17. Rohani S, Trifkovic M, Sheikhzadeh M. Kinetics estimation and single and multi-objective optimization of a seeded, anti-solvent, isothermal batch crystallizer. *Ind Eng Chem Res*. 2008;47(5):1586–1595.
18. Sarkar D, Rohani S, Jutan A. Multi-objective optimization of seeded batch crystallization processes. *Chem Eng Sci*. 2006;61(16):5282–5295.
19. Choong KL, Smith R. Optimization of batch cooling crystallization. *Chem Eng Sci*. 2004;59(2):313–327.
20. Choong KL, Smith R. Optimization of semi-batch reactive crystallization processes. *Chem Eng Sci*. 2004;59(7):1529–1540.
21. Braatz RD, Nagy ZK. Robust nonlinear model predictive control of batch processes. *AIChE J*. 2003;49(7):1776–1786.
22. Nagy ZK, Braatz RD. Worst-case and distributional robustness analysis of finite-time control trajectories for nonlinear distributed parameter systems. *IEEE Trans Control Syst Technol*. 2003;11(5):694–704.
23. Braatz RD, Ma DL, Chung SH. Worst-case performance analysis of optimal batch control trajectories. *AIChE J*. 1999;45(7):1469–1476.

24. Ward JD, Mellichamp DA, Doherty MF. Choosing an operating policy for seeded batch crystallization. *AIChE J*. 2006;52(6):2046–2054.
25. Jagadesh D, Kubota N, Yokota M, Sato A, Tavare NS. Large and mono-sized product crystals from natural cooling mode batch crystallizer. *J Chem Eng Jpn*. 1996;29(5):865–873.
26. Kubota N, Doki N, Yokota M, Sato A. Seeding policy in batch cooling crystallization. *Powder Technol*. 2001;121(1):31–38.
27. Doki N, Kubota N, Yokota M, Chianese A. Determination of critical seed loading ratio for the production of crystals of uni-modal size distribution in batch cooling crystallization of potassium alum. *J Chem Eng Jpn*. 2002;35(7):670–676.
28. Mullin JW, Nyvlt J. Programmed cooling of batch crystallizers. *Chem Eng Sci*. 1971;26(3):369–377.

Manuscript received Oct. 17, 2011, revision received Mar. 11, 2012, and final revision received May 18, 2012.